J Solid State Electrochem (2010) 14:2235–2240
DOI 10.1007/s10008-010-1058-0

ORIGINAL PAPER

Electrodeposition behavior of Mg with Zn from acidic sulfate solutions

Mou Cheng Li · Sen Sen Xin · Ming Yu Wu

Received: 17 December 2009 / Revised: 17 March 2010 / Accepted: 21 March 2010 / Published online: 14 April 2010

Abstract Electrodeposition of Mg with Zn in acidic sulfate solutions with polyethylene glycol and octadecyl dimethyl benzyl ammonium chloride as additives was investigated by scanning electron microscopy, X-ray diffraction, and potentiodynamic polarization techniques. The results show that these two compounds act in a synergetic way to suppress Zn deposition markedly and facilitate Mg reduction. Zn–0.46%Mg coatings are produced under high cathodic current densities, which have lower corrosion potentials than Zn coatings and hydrogen evolution in neutral chloride solutions. Magnesium hydroxide may cause current oscillations at high cathodic polarizations in plating solutions without zinc salts due to its formation and peel-off. An "induced co-deposition" mechanism is proposed for Zn–Mg alloy electrodeposition.

Keywords Electrodeposition · Zinc · Magnesium · Additive · Induced co-deposition

Introduction

Zinc coating is widely used to protect steels from corrosion through hot-dipping or electrodeposition techniques. For example, galvanized steels are the most popular materials in the field of automobiles, buildings, electric appliances, etc. Zinc coating acts optimally as not only sacrificial anode but also barrier to protect steel substrate from corrosion. In order to extend the lifetime, it is of great significance to improve the corrosion resistance of Zn coating. In the literature, alloying elements were often adopted to produce zinc alloy coatings with better corrosion resistance than pure zinc coating, such as Zn–Ni, Zn–Co, Zn–Fe, Zn–Al, and even Zn–Mn coatings. Recently, Mg-alloyed zinc coatings (i.e., Zn–Mg coating) have attracted great attention due to excellent corrosion resistance [1–3], which may come to be the next generation of galvanized steel.

Zn–Mg coatings can be produced through conventional coating techniques such as hot-dipping, physical vapor deposition (PVD), and electrodeposition. Nishimura et al. [4] prepared Zn–Mg coatings with about 0.2% Al by hot-dipping. The corrosion resistance in salt spray test increased greatly with a small amount of Mg added into Zn coatings but changed slightly after Mg content reached 0.5% and up to 2%. The intermetallic phases (e.g., $MgZn_2$ and Mg_2Zn_{11}) in Zn–Mg coating possibly led to the formation of a more densely packed corrosion product layer on coating surface, which enhanced the corrosion resistance. PVD methods are of industrial interest for producing Zn–Mg coatings. Schumacher et al. [5] presented a pilot line to deposit thin PVD metallic coatings on galvanized steel with line production speed up to 60 m/min. Generally, thin Mg film was deposited on a Zn-plated steel surface [6]. Zn–Mg alloy coating was subsequently formed through thermal alloying treatment over 250 °C which promoted inter-diffusion of Mg and Zn and formation of intermetallic phases. To control the coating microstructure, Shedden et al. [7] prepared Zn–Mg coatings by unbalanced magnetron sputtering of pure Zn/Mg targets without further thermal treatment, but the preferential resputtering of Mg would take place.

Electrodeposition is a traditional method to produce metallic coatings. Morishita et al. [8, 9] obtained Zn–Mg coatings by electrodepositing Mg on Zn-plated steels in molten salt. The Zn–Mg alloying process happened during

M. C. Li (✉) · S. S. Xin · M. Y. Wu
Institute of Materials, Shanghai University,
149 Yanchang Road,
Shanghai 200072, China
e-mail: mouchengli@shu.edu.cn

the deposition. In salt spray test, Mg-alloyed Zn coatings had about ten times higher resistance to generate red rust than conventional Zn coatings. However, this molten salt electrolysis is impossible to be put to industrial use. As for requirement of continuous line production and low cost, electrodeposition from aqueous solutions just like Zn coatings may be better for producing Zn–Mg coatings. A big challenge for Zn–Mg alloy electroplating is the standard electrode potential of Mg ($E^{\theta} = -2.34\ V_{SHE}$), far lower than the electrode potentials of Zn and H_2 in aqueous bath. Recently, Nakano et al. [10] found that Zn electrodeposition and hydrogen evolution were suppressed effectively by using quaternary ammonium salt as additive in acidic sulfate solutions, which allowed the co-deposition of Mg with Zn under high cathodic current density conditions. The occurrence of red rust in salt spray test was five times longer for electroplated Zn–0.4%Mg coating than Zn coating on steel. Nevertheless, the additive was burnt easily on the coating surface due to the high deposition current densities.

There is very few information on the Zn–Mg electrodeposition. The aim of this study is to prepare Zn–Mg coating on the basis of continuous electroplating line for steel plates and have an insight into the deposition mechanism in acidic sulfate solutions with quaternary ammonium salt and polyethylene glycol as additives.

Experimental

Electrolytic cell and sulfate-plating bath

Zn–Mg alloy electrodeposition was carried out in a two-electrode cell containing 200 mL sulfate plating solution. A platinum foil served as the anode. Cold-rolled low-carbon steel specimens were used as the cathode with an exposed surface area of about 0.2 cm^2 (i.e., electrodes with a dimension of 4×5 mm). Prior to each plating experiment, the specimen surface was ground with 800 grit waterproof abrasive paper and then pickled in 10% H_2SO_4 at room temperature for 30 s. The anode and cathode were fixed with a space of about 5 cm and immersed vertically into the plating solution about 3 cm lower than the solution surface. The plating solutions were maintained at 60±2 °C and agitated slowly by a magnetic stirrer. The pH value was adjusted to about 1 by diluting with H_2SO_4. Polyethylene glycol (PEG) with a mean molecular weight of 20,000 g mol^{-1} and octadecyl dimethyl benzyl ammonium chloride (OC) were used separately or together as additives. The studied solutions were listed as follows:

S_B $ZnSO_4{\cdot}7H_2O$ (50 g L^{-1}) + $MgSO_4{\cdot}7H_2O$ (200 g L^{-1}), the base solution

S_O S_B + OC

S_P S_B + PEG

S_{OP} S_B + OC + PEG

S_{Mg} removing $ZnSO_4{\cdot}7H_2O$ from S_{OP}

In all cases, the concentrations of PEG and OC were 1 g L^{-1}. All chemicals were of analytical grade. Distilled water was used to make these solutions.

Electrodeposition procedure

Zn–Mg coatings were prepared through direct current plating with a current density of 2 A cm^{-2} for 1 min. PAR (Princeton Application Research, AMETEK Inc.) system, which comprised an M273A potentiostat/galvanostat and the PowerSuite software, was used to supply direct current.

Cathodic polarization curves were determined potentiodynamically with a potential scan rate of 2 mV s^{-1} in the aforesaid electrolytic cell using a saturated calomel electrode (SCE) as the reference electrode. Each curve was corrected for ohmic potential drop deduced from the high-frequency electrode impedance. Potentiodynamic scans and impedance measurements were conducted using the above PAR system.

Characterization of coatings

The surface morphology of electrodeposits were observed using scanning electron microscopy (SEM) (JSM 6700F). X-ray diffraction (XRD) analysis was conducted by using a Rigaku diffractometer (D/MAX 2550 V) with CuKα irradiation (λ=0.15405 nm). The scanning rate was 6°/min for 2θ ranging from 30° to 90°. The Zn and Mg contents of coatings were determined by atomic absorption spectrophotometer (AAS; SPQ-800). The corrosion potential method was used to characterize pure Zn and Zn–Mg coatings in neutral 3.5% NaCl solutions.

Results

Effect of additives on electrodeposition

Figure 1 gives the potentiodynamic polarization curves in all test solutions, which indicated that the organic additives had great influence on cathodic polarizations. In solution S_B without any additive, a current density peak appeared at about −0.94 V_{SCE}, which was related to the hydrogen evolution and formation of adsorbates (e.g., $ZnOH_{ad}$ and ZnO_{ad}). After this peak, a quasi-plateau existed in the potential range −1.05 to −1.12 V_{SCE}, which revealed that the hydrogen evolution resulted in the accumulation of adsorbates [11–14]. Zinc started to deposit at about −1.12 V_{SCE}. The further decrease of

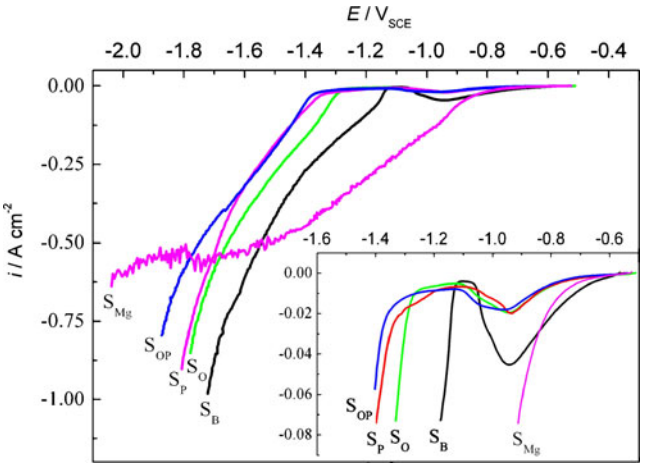

Fig. 1 Polarization curves for steel electrodes in different solutions. The *inset* shows the low current density part

electrode potential would accelerate the Zn deposition and hydrogen evolution.

In comparison with S_B, the solutions S_O, S_P, and S_{OP} showed lower hydrogen evolution peaks, wider potential ranges for accumulating processes of adsorbates, and much lower onset potentials for zinc deposition (i.e., about −1.26, −1.33, and −1.36 V_{SCE}, respectively). These indicated that both OC and PEG had a strong inhibiting effect on the hydrogen reduction and zinc deposition potential, and there was a little synergetic effect between them to reduce the zinc deposition potential. Furthermore, polarization curves in S_P and S_{OP} almost overlapped at low current densities ranging from about −0.1 to −0.3 A cm^{-2} but separated at higher current densities. As current density increased to about −0.5 A cm^{-2}, the polarization curve in S_P approached to that in S_O. Obviously, the synergetic effect between OC and PEG shifted the electrode potential to lower values than the single ones under high current density conditions. The data with current density larger than about −0.8 A cm^{-2} were deleted in view of the marked ohmic drop. It could be inferred that the electrode potential at −2 A cm^{-2} for electrodepositing from S_{OP} should be much lower than those in S_O and S_p, which would be favorable to achieving Mg deposition on electrochemical principle.

The coatings electrodeposited at −2 A cm^{-2} for 1 min were dissolved by dilute nitric acid, and the weight contents of Zn and Mg in coatings were analyzed by using AAS. Zn deposition decreased from 9.95 to 5.80, 5.06, and 4.48 mg cm^{-2} upon adding OC, PEG, and both compounds into the base solutions, respectively. It is obvious that PEG is a little more inhibitive than OC to zinc electrodeposition and a synergetic effect exists between them, which are consistent with polarization behavior in Fig. 1. On the contrary, the Mg deposition increased from 0.8 to 4.80, 4.55, and 20.6 μg cm^{-2}, respectively, with the addition of the above additives. Moreover, as calculated, weight percentage of Mg in coatings was less than 0.01% for S_B, indicative of almost no Mg deposition without additives. With single addition of OC or PEG, Mg content was no more than 0.1%, but their combination in S_{OP} led to a higher Mg content at about 0.46%.

Influence of sulfate zinc content on polarization

In order to elucidate the Zn–Mg co-deposition, polarization behavior was further investigated in solution S_{Mg} containing no zinc salt, as shown in Fig. 1. Compared with S_{OP}, S_{Mg} had the same additives, but only magnesium salt. The current density in S_{Mg} increased linearly from about −0.9 to −1.5 V_{SCE} and thereafter increased slowly in the company of oscillations. As discussed later, these may be related with hydroxide adsorbates $Mg(OH)_2$ and hydrogen evolution. After the measurement of polarization curve up to −2.2 A cm^{-2} in S_{Mg}, no deposits were observed on the electrode surface, indicating that Mg was not electrodeposited from S_{Mg} without zinc salt.

Surface characterization of Zn–Mg coatings

Zn–Mg coatings deposited from S_{OP} showed metallic luster and were characterized by surface analysis techniques. SEM observation in Fig. 2 found that the coating was composed of thin flakes with thickness less than 40 nm. The growth process was mainly dominated by Zn deposition because only 0.46% Mg co-deposited with Zn. The cross-section image shows that the Zn–Mg coating was dense and attached tightly to the steel substrate.

XRD analysis in Fig. 3 found intermetallic phase Mg_2Zn_{11} in the coating. It can be inferred from Mg content that the coating only had a small quantity of Mg_2Zn_{11}. Thus, its response peaks were weak and almost merged with those of Zn. Furthermore, no carbon peak was observed because organic additives were not burnt during electrodeposition.

Corrosion potential of coatings

Zn–Mg and Zn coatings were immersed in 3.5% NaCl solutions at 25 °C. Figure 4 gives the variation of their corrosion potentials with immersion time. Zn coating reached a steady corrosion state quickly at about −1.05 V_{SCE}, whereas the corrosion potential of Zn–Mg coating showed a drop within 20 min and then stabilized slowly at about −1.07 V_{SCE}. This steady value was about 20 mV lower than that of Zn coating. Additionally, a few bubbles were observed on Zn–Mg coating surface during the initial immersion, which could be attributed to hydrogen evolution at the electrode potentials lower than −1.08 V_{SCE}. These results revealed that Mg existed mainly as metallic state in the alloy coating

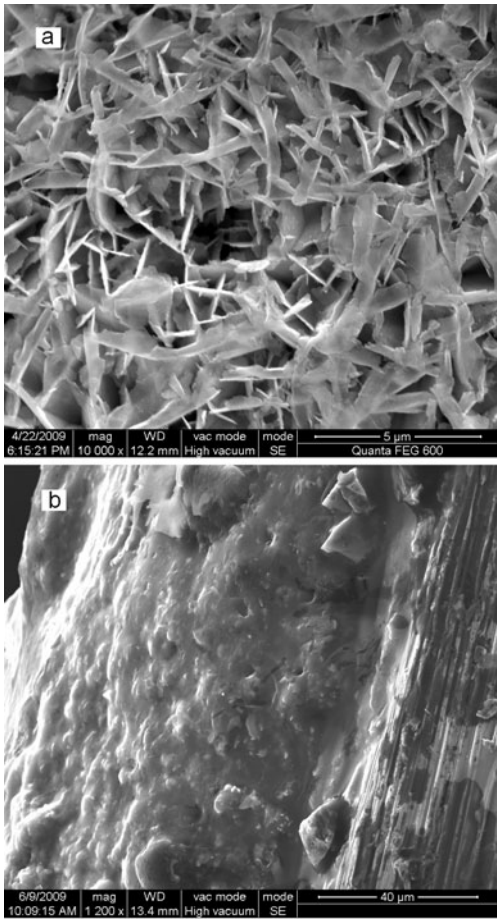

Fig. 2 SEM morphologies for **a** the surface and **b** cross-section of Zn–Mg coatings electrodeposited from solution S_{OP}

instead of ionic state. Hausbrand et al. [15] also observed much lower corrosion potentials for intermetallic $MgZn_2$ than zinc in chloride solutions. Further work is ongoing to elucidate the corrosion behavior of Zn–Mg alloy coatings.

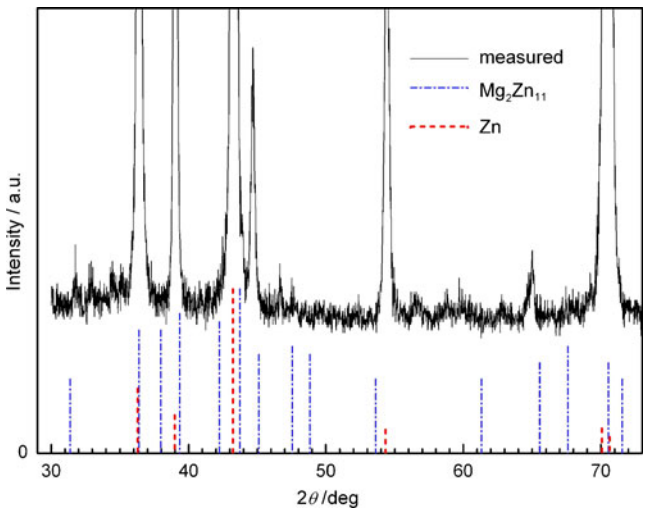

Fig. 3 XRD pattern for Zn–Mg deposits obtained from solution S_{OP}

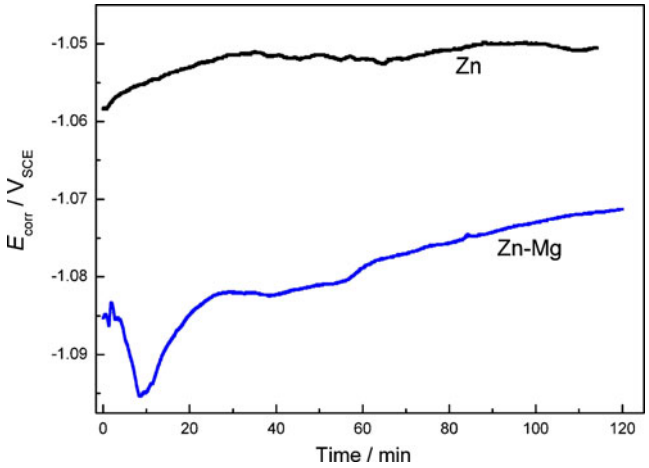

Fig. 4 Time dependence of corrosion potentials for Zn–Mg and Zn coatings in 3.5% NaCl solutions

Discussion

Synergetic effect between OC and PEG

In order to achieve the co-deposition of Mg and Zn, it is very important to increase the cathodic polarization of Zn deposition and suppress the hydrogen evolution because of the marked difference between the electrode potentials of their reduction reactions in aqueous solutions. Organic additives such as OC and PEG are often used in zinc plating baths to inhibit the reduction reactions. As a type of cationic surfactant, OC can adsorb strongly onto cathode surfaces (especially the active sites) through electrostatic force to hinder the reduction reactions [16, 17], but it presumably blocked only a partial surface area due to its relatively small molecular volume, which maybe was the main reason for the lower polarization effect in S_O (Fig. 1). Comparatively, PEG has a very big molecular volume and can adsorb more or less evenly to form a barrier layer with a well-ordered structure on the electrode surface [18, 19]. Just due to this good blocking effect, the onset of zinc deposition was shifted to more negative potentials in S_P. Nevertheless, as a result of nonionic nature, PEG maybe desorbed partly from the electrode surface with increasing the cathodic current density to higher than −0.5 A cm^{-2} because of the violent evolution of hydrogen bubbles. Such behavior was also observed by other authors during zinc electrodeposition [16, 19]. This was responsible for the decreased polarization effect under high current densities in S_P (Fig. 1).

A mixture of OC and PEG created higher overpotentials under high cathodic current densities than single OC or PEG. The synergetic effect between them had been scarcely investigated in the deposition process of zinc and other metals, which resulted in co-deposition of Zn and Mg here. Its mechanism must relate with interaction between OC and PEG through co-adsorption, even their associates. As

coexisted with PEG in solutions, OC could provide both halide ions Cl^- to induce a better adsorption of PEG molecules as observed in Cu and Zn depositions [14, 20–23] and electrostatic force to overcome the desorption that resulted from strong hydrogen evolution [16]. At the same time, PEG could offset the low blocking issue of OC with its huge molecules. Thus, OC/PEG mixed additives would form a continuous barrier layer on cathode surface under high current densities to suppress Zn deposition.

To show the inhibitive effect of additives, current efficiency of deposition was calculated with the coating mass. Its value decreased in the order of S_B, S_{OC}, S_P, and S_{OP} (i.e., 24.6%, 14.3%, 12.5%, and 11.2%) due to the gradually increased blocking effect of additives.

Mechanism for electrodepositing Zn–Mg alloy

Similar to the effect of $Zn(OH)_2$ on low cathodic polarizations of Zn electrodeposition [12], forming magnesium hydroxide $Mg(OH)_2$ on electrode surface could hinder hydrogen evolution to a certain extent. The polarization behavior and oscillations in S_{Mg} after −1.5 V_{SCE} (Fig. 1) may be attributed to the competition between formation and peel-off of both adsorbates $Mg(OH)_2$ and hydrogen bubbles. However, as for S_{OP}, a small amount of $Mg(OH)_2$ would co-deposit with Zn and incorporate into Zn electrodeposits, instead of peeling off. Therefore, Mg deposition might take place through the reduction of $Mg(OH)_2$.

Though Mg had been deposited in metallic state by Nakano [10], no mechanism is established for the reduction of Mg^{2+} ions from aqueous solutions in the literature. According to the above results and analysis, the following "induced co-deposition" is proposed for Zn–Mg alloy electrodeposition at high cathodic polarizations:

$$Zn^2 + e \rightarrow (Zn^+)_{ad} \quad (1)$$

$$(Zn^+)ad + e \rightarrow Zn \quad (2)$$

$$Zn + H^+ + e \rightarrow ZnH_{ad} \quad (3)$$

$$ZnH_{ad} + H^+ + e \rightarrow Zn + H_2 \quad (4)$$

$$Mg^{2+} + 2OH^- \rightarrow \left[Mg(OH)_2\right]_{ad} \quad (5)$$

$$7Zn + 4ZnH_{ad} + 2\left[Mg(OH)_2\right]_{ad} \rightarrow Mg_2ZN_{11} + 4H_2O \quad (6)$$

where the subscript "ad" represents the adsorbates formed during the deposition as intermediate species. The reduction of Zn^{2+} ions is simply written as shown in Eqs. 1 and 2 but may also include $[Zn(OH)_2]_{ad}$ and more intermediates [11, 24]. Just like the "induced co-deposition" of tungsten and molybdenum with iron group metals [25–29], reduction of Mg^{2+} ions may include two steps, i.e., $[Mg(OH)_2]_{ad}$ forming on electrode surface and then reduced by adsorbed hydrogen ZnH_{ad}. The strong hydrogen evolution through reactions 3 and 4 will not only lead to $[Mg(OH)_2]_{ad}$ precipitation in Eq. 5 due to increasing the interfacial pH but also provide adsorbed hydrogen atoms to reduce $[Mg(OH)_2]_{ad}$ in Eq. 6. Obviously, a lower current efficiency means a faster hydrogen evolution, which may result in a higher interfacial pH to facilitate the formation and reduction of $[Mg(OH)_2]_{ad}$. This is mainly responsible for a relatively higher Mg content in the coatings electrodeposited from S_{OP}.

Conclusions

Mg^{2+} ions cannot be reduced in additive-free acidic sulfate solutions. Organic compounds PEG and OC, used separately or together as additives, have a great effect on the cathodic polarization process. Compared with the single ones, a mixture of PEG and OC can shift zinc deposition potentials to more negative values. The synergetic effect between them creates a continuous barrier layer on the electrode surface and sufficiently suppresses zinc deposition under high current densities. As a result, Zn–0.46%Mg coatings are electrodeposited at −2 A cm^{-2} without burnt characteristics.

The current oscillations appear in the solutions without zinc sulfate. Mg co-deposits with Zn at high cathodic polarizations and may follow the induced co-deposition mechanism. The co-deposition includes two steps: adsorbates $[Mg(OH)_2]_{ad}$ incorporated into Zn electrodeposits and then reduced by adsorbed hydrogen. Compared with Zn coating, Zn–Mg coating shows lower corrosion potentials and hydrogen evolution in neutral chloride solutions, which confirms the existence of Mg in metallic state such as intermetallic Mg_2Zn_{11}.

Acknowledgements Financial support provided by the Natural Science Foundation of China (NSFC, grant no. 50771109) and Shanghai Municipal Education Commission (09YZ21) is greatly appreciated.

References

1. Hosking NC, Strom MA, Shipway PH, Rudd CD (2007) Corros Sci 49:3669
2. Volovitch P, Allely C, Ogle K (2009) Corros Sci 51:1251

3. Prosek T, Nazarov A, Bexell U, Thierry D, Serak J (2008) Corros Sci 50:2216
4. Nishimura K, Shindo H, Nomura H, Katoh K (2003) Tetsu to Hagane 89:174
5. Schuhmacher B, Schwerdt C, Seyfert U, Zimmer O (2003) Surf Coat Technol 163–164:703
6. Lee MH, Kim JD, Oh JS, Yang JH, Naek SM (2008) Surf Coat Technol 202:5590
7. Shedden BA, Katardjiev IV, Berg S, Samandi M, Window B (1999) Surf Coat Technol 116–119:751
8. Morishita M, Koyama K, Murase M, Mori Y (1996) ISIJ Int 36:714
9. Morishita M, Koyama K, Mori Y (1997) ISIJ Int 37:55
10. Nakano H, Oue S, Kobayashi S, Fukushima H, Araga K, Okumura K, Shige H (2004) Tetsu-to-Hagane 90:51
11. Cachet C, Wiart R (1994) J Electrochem Soc 141:131
12. Yan H, Downes J, Boden PJ, Harris SJ (1996) J Electrochem Soc 143:1577
13. Gomes A, da Silva Pereira MI (2006) Electrochim Acta 51:1342
14. Li MC, Luo SZ, Qian YH, Zhang WQ, Jiang LL (2007) J Electrochem Soc 154:D567
15. Hausbrand R, Stratmann M, Rohwerder M (2009) Corros Sci 51:2107
16. Hsieh JC, Hu CC, Lee TC (2008) J Electrochem Soc 155:D675
17. Ortiz-Aparicio JL, Meas Y, Trejo G, Ortega R, Chapman TW, Chainet E, Ozil P (2008) J Electrochem Soc 155:D167
18. Lee JY, Kim JW, Lee MK, Shin HJ, Kim HT, Park SM (2004) J Electrochem Soc 151:C25
19. Kim JW, Lee JY, Park SM (2004) Langmuir 20:459
20. Trejo G, Ruiz H, Ortega R, Meas Y (2001) J Appl Electrochem 31:685
21. Bahena E, Mendez PF, Meas Y, Ortega R, Salgado L, Trejo G (2004) Electrochim Acta 49:989
22. Bonou L, Eyraud M, Denoyel R, Massiani Y (2002) Electrochim Acta 47:4139
23. Kelly JJ, West AC (1998) J Electrochem Soc 145:3477
24. Cachet C, Wiart R (1999) Electrochim Acta 44:4743
25. Franklin TC (1987) Surf Coat Technol 30:415
26. Ibrahim MAM, el Rehim SS Abd, Moussa SO (2003) J Appl Electrochem 33:627
27. Podlaha EJ, Landolt D (1996) J Electrochem Soc 143:839
28. Crousier J, Eyraud M, Crousier JP, Roman JM (1992) J Appl Electrochem 22:749
29. Tsyntsaru N, Bobanova J, Ye X, Cesiulis H, Dikusar A, Prosycevas I, Celis JP (2009) Sur Coat Technol 203:3136